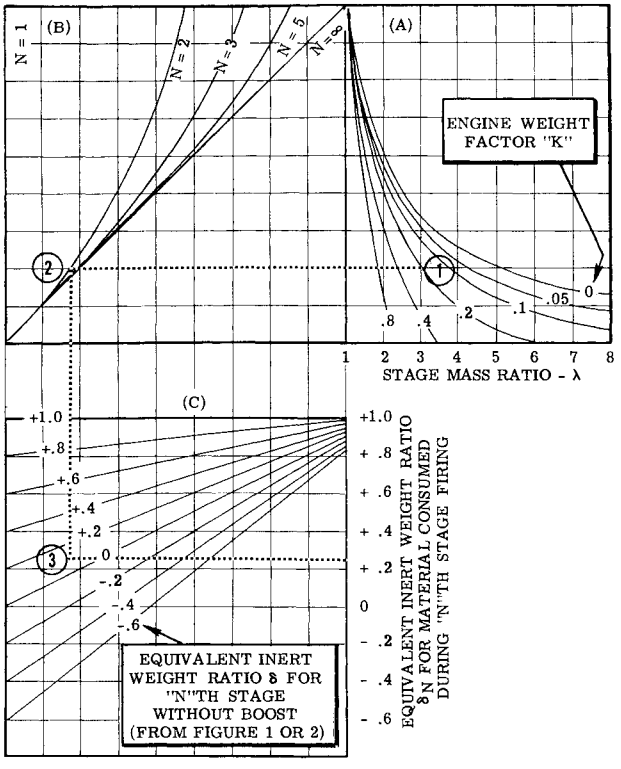

Fig. 3 Equivalent inert weight ratios for the *N*th stage engine—all stages having the same mass ratio, engine weight factor, and specific impulse.

ing the ratios of effective specific impulses among the stages. The curves and equations are therefore considered valid for all rockets having essentially ballistic trajectories.

The curves of Figs. 1 and 2 focus attention on the role of axial specific impulse in establishing equivalent inert weight. Determination of the axial specific impulse may be difficult because of the difficulty of evaluating the marginal thrust increments associated with expenditures of small quantities of materials. In the case of the injection thrust vector control system, axial thrust components are readily approximated so this is not a problem.

The magnitudes of the equivalent inert weight ratios which the curves and equations establish, show that these ratios should be used when comparing weights of systems involving expendable materials. The preceding equations and curves provide a convenient means of approximating the values of the ratios for systems studies and design analyses.

Single-Plane Simulation of a Rolling Missile

ROBERT E. JOFFS*
U. S. Naval Ordnance Laboratory, Corona, Calif.

A SINGLE-PLANE simulation has been employed in investigations of roll rate, control surface response techniques, missile glide angle, and missile navigation schemes.

Presented at the AIAA Simulation for Aerospace Flight Conference, Columbus, Ohio, August 26–28, 1963; revision received December 11, 1963.

* Senior Project Engineer, Dynamics Division.

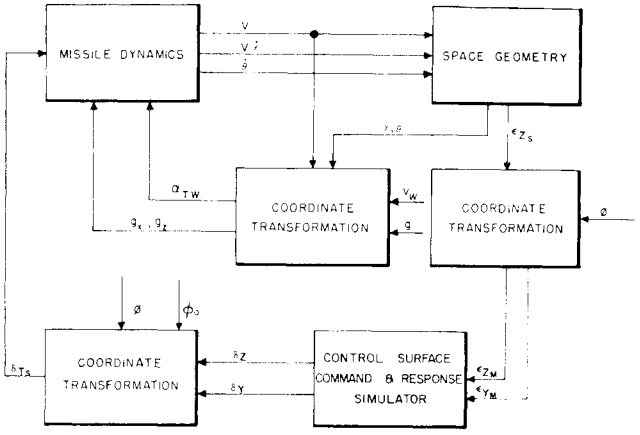

Fig. 1 Mechanization block diagram.

Because of its simplicity, it cannot be used to examine such factors as cross coupling, gyro drift errors, and cross talk from control surface deflections (evaluation of these requires a more complex simulation); but it does provide a means of examining certain missile performance characteristics more readily and more rapidly than is possible with three-dimensional simulations.

Figure 1 shows the relationship of the various elements of the simulation, which is performed on an electronic analog computer. The physical equipment required to perform the simulation is as follows: 49 summing amplifiers, 17 integrating amplifiers, 2 resolvers, 5 channels of electronic multipliers, 9 servo multipliers, 6 function generators, and 6–10 recording channels.

Simulation

The missile is simulated by describing it with lateral and longitudinal force equations and the pitch moment equation as follows:

$$m\dot{V} = \Sigma F_X - mg \sin\gamma \qquad (1)$$

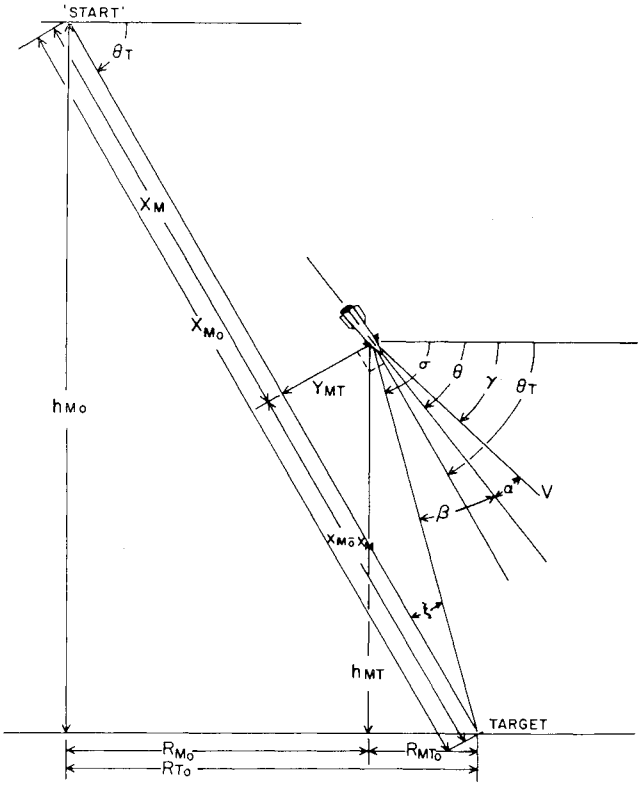

Fig. 2 Geometric relationships.

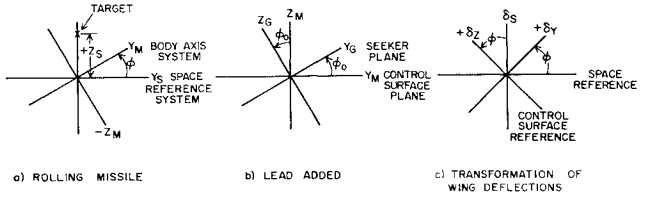

Fig. 3 Geometric relationships.

$$mV\dot{\gamma} = \Sigma F_Z - mg\cos\gamma \tag{2}$$

$$\dot{Q} = m'/I_{YY} \tag{3}$$

where

$$m' = Sqd[C_{m_\alpha}(\alpha + \alpha_W) + C_{M_{\delta_\alpha}}\delta_s] - \left(\frac{Sd}{2}\right)\left(\frac{C_{m_\theta}}{V}\right)\left(1481\lambda\,\frac{M2}{V_s}\right)\dot{\theta} \tag{4}$$

$$\Sigma F_X = -Sq[C_A + \Delta C_{D\delta}(|\delta_{X_M}| + |\delta_{Z_M}|)] \tag{5}$$

$$\Sigma F_Z = SqC_{N_\alpha}(\alpha + \alpha_W) \qquad q = 1481\lambda M^2 \tag{6}$$

The basic geometric relationships used were selected to provide maximum accuracy in the final miss-distance readout. The miss distance is measured perpendicularly from the initial line-of-sight to the target. This technique allows a maximum scale factor of 1 v = 4 ft, which gives a satisfactory degree of precision for the miss-distance measurement. The following equations describe, respectively, the geometric relationships shown in Fig. 2:

$$h_{MT_0}, R_{MT_0}, X_{MT_0}, Y_{MT_0}, = -h_{M_0}, R_{T_0}, X_{T_0}, -Y_{M_0} \tag{7}$$

$$\dot{h}_{MT} = \dot{h}_M = V\sin\gamma \tag{8}$$

$$\dot{R}_{MT} = \dot{R}_M = V\cos\gamma \tag{9}$$

$$\dot{X}_{MT} = \dot{X}_M = V\cos(\theta_T - \gamma) \tag{10}$$

$$\dot{Y}_{MT} = \dot{Y}_M = V\sin(\theta_T - \gamma) \tag{11}$$

$$h_{MT} = h_{MT_0} - \int \dot{h}_{MT}\,dt = -h_{M_0} - \int V\sin\gamma\,dt \tag{12}$$

$$R_{MT} = R_{MT_0} - \int \dot{R}_{MT}dt = R_{T_0} - \int V\cos\gamma\,dt \tag{13}$$

$$X_{MT} = X_{MT_0} - \int \dot{X}_{MT}dt = X_{T_0} - \int V\,dt \tag{14}$$

$$Y_{MT} = Y_{MT_0} - \int \dot{Y}_{MT}dt = Y_{M_0} - \int V(\theta_T - \gamma)dt \tag{15}$$

For pursuit, $\epsilon = \beta$; for constant bearing, $\epsilon = \theta_T - \theta - \beta$; and for deviated pursuit, $\epsilon = \beta + \beta_S$ and $\theta = \alpha - \gamma$.

The control surface deflections (δ_Z and δ_Y) in Eqs. (4) and (5) are simulated as follows. Error signals from the missile seeker are fed to a guidance computer which generates control surface commands for bang-bang deflections. Each up-down or right-left command is generated for a period of time which is a function of the roll rate and the amount of control surface deflection required, which can either be arbitrarily chosen within the limits of satisfactory performance or can be made a function of the target error angle. By making the control surface deflection a function of the target error angle, there is obtained a quasi-proportional type of control system in which the normal acceleration generated by the deflection is proportional to the magnitude of the target error angle. Flights showing both types of control

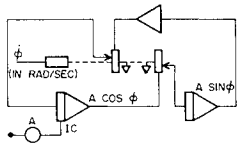

Fig. 4 Roll mechanization.

systems have been studied. The commands are square wave pulses that are fed into a response simulator circuit.

The error angles are introduced into the rolling missile system using the geometric relationships of Fig. 3a. From these relationships and the fact that the error angle in the space reference system is in the XZ plane and the distance to target (X) is approximately the same as it is for the rolling missile reference system if small error angles are assumed, the error angle in the missile reference system is

$$\epsilon_{YM} = \tan^{-1}Z_s(\sin\varphi)/X_s \tag{16}$$

and

$$\epsilon_{ZM} = \tan^{-1}Z_s(\cos\varphi)/X_s \tag{17}$$

In the space reference system, assuming small error angles,

$$\epsilon_{Z_s} = Z_s/X_s \tag{18}$$

and for the small angles in the missile reference system

$$\epsilon_{YM} \simeq \epsilon_{Z_s}\sin\varphi \qquad \epsilon_{ZM} \simeq -\epsilon_{Z_s}\cos\varphi \tag{19}$$

The $\sin\varphi$ and $\cos\varphi$ terms are generated by means of an undamped oscillator whose frequency is changeable (Fig. 4). The roll rate $\dot{\varphi}$ is generated as a function of Mach number when the specific study requires no greater accuracy than is provided by this method, or by some other method when greater accuracy is required.

To compensate for the lag in the control surface response, lead may be added to the error angle by simply rotating the seeker plane a fixed angle φ_0 from the wing plane (Fig. 3b). The target error angle then becomes

$$\epsilon_{YM} = \epsilon_{Z_s}\sin(\varphi + \varphi_0) \text{ and } \epsilon_{ZM} = \epsilon_{Z_s}\cos(\varphi + \varphi_0) \tag{20}$$

or

$$\epsilon_{ZM} = (\cos\varphi\cos\varphi_0 - \sin\varphi\sin\varphi_0) \tag{21}$$

Since φ_0 was assumed constant, $\cos\varphi_0 = K_1$ and $\sin\varphi_0 = K_2$, then

$$\epsilon_{ZM} = \epsilon_{Z_s}(K_1\cos\varphi - K_2\sin\varphi) \tag{22}$$

and the same applies for ϵ_{YM}.

These relationships are mechanized on the computer by multiplying the outputs of the roll oscillator by scale potentiometers set at K_1 and K_2 and summing them in summing amplifiers. The error angles generated in the space referenced system have now been resolved into the rolling missile reference system, and a lead has been added to compensate for the lag in control surface response. The error angles are sent to a threshold detector and command generation circuit, and the commands are fed into the control surface response circuit. The resulting wing deflections are transformed into the space reference system (see Fig. 3c), from which it can be seen that the control surface deflection in the XZ plane of the space reference system is $\delta_s = \delta_Y\sin\varphi + \delta_Z\cos\varphi$; with this, the missile dynamics are solved, and the resulting accelerations are used to solve the kinematics (Fig. 1).

Results and Conclusions

Studies have been made of the terminal phase of flight (last 3–5 miles), and miss distances have been determined for flights incorporating systematic variations in lead angle, flight-path angle, magnitude of the error-angle threshold at which control surface commands are triggered, length of time the wing surfaces are held hardover, different types of navigation schemes, and other control system parameters. The degrading effects of boresight errors, wind, loss of error signals, and movement of the source of error signals have also been assessed.

Shown in Figs. 5 and 6 are oscillograph recordings obtained during two typical simulated flights. Figure 5 recordings were

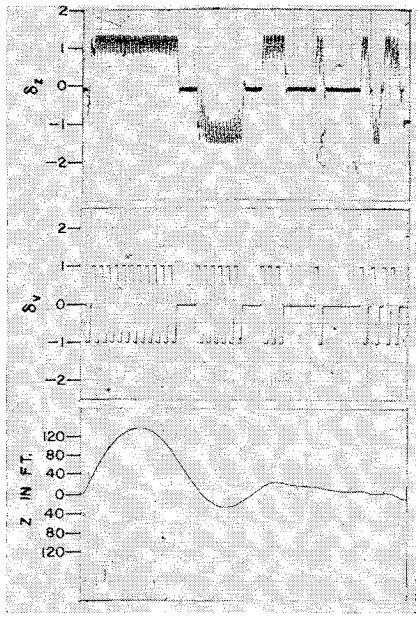

Fig. 5 Record of bang-bang control flight.

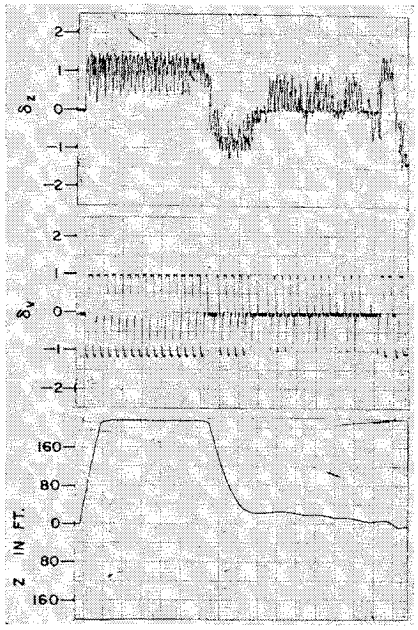

Fig. 6 Record of proportional control flight.

made from a simulated flight using a bang-bang type of control system, in which the length of time that control surfaces are deflected is constant. For this particular flight, the control surface deflection time was made equal to the time the missile requires to roll 150°. The recordings of Fig. 6 were made from a simulated flight using a proportional type of control system in which the length of time the control surfaces are deflected is proportional to the magnitude of the target error angle. The δ_Y recordings are made with respect to the rolling missile axis system and are control surface deflections plotted as a function of time. The δ_Z and Z plots are made with reference to the space-stabilized axis system. The δ_Z is the effective control surface deflection in the pitch plane plotted as a function of time, and Z is the plot of missile trajectory.

In conclusion, the single-plane simulation of a rolling missile has made possible the optimization of a large number of system characteristics, and the simplicity of the simulation makes it easy to set up, check out, and make changes.

Explicit Rendezvous Guidance Mechanization

THOMAS L. GUNCKEL II*
North American Aviation, Inc., Anaheim, Calif.

THIS paper presents a set of guidance equations based on an exact solution of the equations of motion of the rendezvous vehicle. The rendezvous is accomplished in two thrusting periods: injection into the rendezvous trajectory, and nulling the closing velocity. By selecting the time of rendezvous, a free-fall trajectory may be determined which starts at the present position of the vehicle and passes through the rendezvous point at the designated time. The guidance system determines the velocity required to achieve this free-fall trajectory, and drives the difference between the required and the actual velocity to zero. When the required velocity is achieved, the engines are cut off, and the vehicle coasts to rendezvous. Near the rendezvous point the engines are reignited to null the closing velocity. The terminal phase of rendezvous is already discussed adequately in the literature.[1, 2] Therefore, this note is concerned mainly with determining the velocity vector necessary to achieve the free-fall trajectory that passes between two points in space in a given time increment.

Gauss' method of orbit determination[3] could be used, but the equations involve numerous functions, which require too much time to solve in updating the required velocity. These time lags affect the accuracy of the updating, the steering loop, and the mechanics of cutoff. To surmount this problem, the mechanization equations discussed in this paper use dual major and minor cycle.

Mechanization Equations

The use of a fixed time of rendezvous means that this trajectory must pass through a given point in space at the rendezvous time. The total time rate of change of the required velocity $\bar{V}_R$ for this maneuver is

$$\frac{d\bar{V}_R}{dt} = \frac{\partial \bar{V}_R}{\partial t} + \left[\frac{\partial \bar{V}_R}{\partial \bar{P}}\right]\frac{d\bar{P}}{dt} \tag{1}$$

where $[\partial \bar{V}_R/\partial \bar{P}]$ is a three-by-three matrix of partial derivatives, $\bar{P}$ is the present position, and $d\bar{P}/dt$ the present velocity $\bar{V}$ of the vehicle. This equation can be put in a slightly different form by noting that, if the vehicle were on the rendezvous trajectory, its velocity would be $\bar{V}_R$ and that the total time rate of change of the required velocity would be the gravitational acceleration:

$$\bar{g} = (\partial \bar{V}_R/\partial t) + [\partial \bar{V}_R/\partial \bar{P}]\bar{V}_R \tag{2}$$

Vehicle steering and engine cutoff will probably be based upon the velocity-to-be-gained $\bar{V}_g$:

$$\bar{V}_g = \bar{V}_R - \bar{V} \tag{3}$$

Noting that the vehicle acceleration can be written as

$$d\bar{V}/dt = \bar{g} + \bar{A}_T \tag{4}$$

where $\bar{A}_T$ is acceleration because of thrust and other nongravitational forces, and combining Eqs. (1–4) yields (see Ref. 4)

$$d\bar{V}_g/dt = -_T \bar{A} - [\partial \bar{V}_R/\partial \bar{P}]\bar{V}_g \tag{5}$$

An explicit mechanization of Eq. (5) would require knowing the partial derivative matrix $[\partial \bar{V}_R/\partial \bar{P}]$ for all possible

Received December 30, 1963.

* Space Analysis Chief, Systems Division, Autonetics.